

Learning Zero-Shot Material States Segmentation, by Implanting Natural Image Patterns in Synthetic Data

Sagi Eppel*^{1,2,4,5}, Jolina Li*^{1,3}, Manuel Drehwald^{1,3}, Alán Aspuru-Guzik^{1,2,3,4}

Abstract

Visual understanding and segmentation of materials and their states is fundamental to understanding the physical world. The myriad textures, shapes, and often blurry boundaries formed by materials make this task particularly hard to generalize. Whether it's identifying wet regions of a surface, minerals in rocks, infected regions in plants, or pollution in water, each material state has its own unique form. For neural nets to learn general class-agnostic material segmentation, it is necessary to first collect and annotate data that captures this complexity. Collecting and manually annotating real-world images is limited by the cost and precision of manual labor. In contrast, synthetic CGI data is highly accurate and almost cost-free, but fails to replicate the vast diversity of the material world. This work offers a method to bridge this crucial gap by implanting patterns extracted from real-world images in synthetic data. Hence, patterns automatically collected from natural images are used to map materials into synthetic scenes. This unsupervised approach allows the generated data to capture the vast complexity of the real world while maintaining the precision and scale of synthetic data. We also present the first general benchmark for zero-shot material state segmentation. The benchmark contains a wide range of real-world images of material states, like food, rocks, construction, plants, liquids, and many others, each in various states (wet/dry/stained/cooked/burned/worn/rusted/sediment/foam, etc.). The annotation includes both partial similarity between regions with similar but not identical materials, and hard segmentation of only points in the exact same material state. We show that net trains on MatSeg significantly outperform existing state-of-the-art methods on this task. The dataset, code, and trained model are available at: [this url](#).

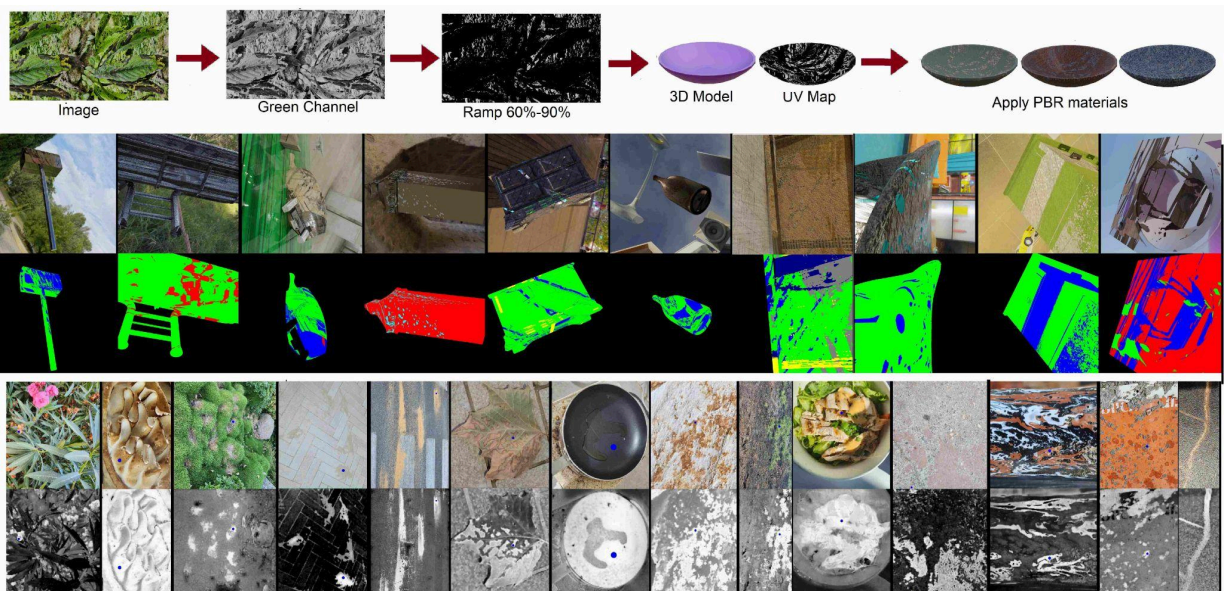


Figure 1) Paper Overview. Top: The procedure for extracting patterns from natural images and implanting them in synthetic scenes. Centre: synthetic dataset and segmentation map. Bottom: real-world images from the material state segmentation benchmark and predicted results for a single material similarity map.

*Equal Contribution. 1. University Of Toronto, 2. Vector Institute, 3. Computer Science Department, 4. Chemistry Department, 5 Innovize Tech. Contact email: Sagieppel@gmail.com

1. Introduction

Materials and their state form a vast amount of shapes and patterns that define the physical and visual world. Wetting of surfaces, minerals on rocks, sediment in soil, corrosion of metals, the rot of food, infections on plants, cracks on walls, stains on fabrics, and phase separation in liquids are some of the almost infinite numbers of patterns formed by materials. Visual understanding separating these states in images is a fundamental part of understanding the physical world. Understanding and mimicking the deep structure and mechanism of every shape and pattern formed by materials encompasses the entire physical sciences and is not feasible. Machine learning, particularly deep neural networks, offers a way to recognize and segment these patterns by learning from extensive annotated data, shifting the focus from understanding each state to collecting sufficient representative data. This task is challenging due to the vast variety of ways materials appear in the world. Two main approaches were used to collect data for this task, the first involved collecting real-world images and using human annotators to segment them into different material regions¹⁻⁴. This approach is limited by the cost of human labor and by the fact that humans perform poorly in segmenting scatter patterns (cracks, drops) as well as soft boundaries and gradual transitions between states⁵. The alternative approach uses synthetic data using CGI and simulation⁶⁻²². This approach has no limitation on the amount of data it can generate and the precision of the annotations but is limited to procedural generation roles that cannot capture the vast complexity and patterns of the real world²³⁻²⁷.

1.1. Implanting Real-World Patterns in Synthetic Data.

In this work, we suggest a way to bridge this critical gap by automatically extracting shapes and patterns from real-world images and using these to map materials on synthetic objects and scenes. This allows us to achieve the precision and scale of synthetic data with the vast variability of patterns in the real world. The core idea is that extracting shapes from images could be easily done by focusing on one main feature, such as intensity, hue, saturation, or one of the R, G, B channels (Figure 2b). Each of these features turns the image into a 2D topological map that can be used to UV map materials onto the surfaces of objects in a synthetic scene (Figure 2). These are then set into a scene and rendered into an image with already-known segmentation maps. Since the map is automatically extracted, it will capture image patterns and shapes without human intervention or previous knowledge about these patterns. The core hypothesis of this approach is that the shapes of materials in the image will not always be mapped into simple features like brightness or hue, but in some specific cases, they will. For example, in some cases, drops on glass, stains on fabric, or minerals in rocks will be significantly brighter or darker, allowing a brightness map to capture their shape. Since we automatically collect patterns from a giant amount of images, it is likely that any important shape or pattern will, in some cases, be correlated with simple properties and will be extracted. Once extracted, this can be used to map any material onto any surface in any scene and therefore be learned by the net in a general setting beyond the setting in which it was extracted (Figures 2–3).

1.2. Zeros-Shot Material States Segmentation Benchmark.

We present the first general benchmark for zero-shot, class-agnostic material state segmentation. The benchmark contains 820 real-world images with a wide range of materials and settings. For example: food states (cooked/burned...), plants (infected/dry.), rocks/soil (minerals/sediment), construction/metals (rusted, worn), liquids (foam/precipitate), and many other states in a class-agnostic manner. The goal is to

evaluate the segmentation of materials without knowledge or pretraining on the material or setting. The focus is on materials with complex or scattered boundaries and gradual transitions (like the level of wetness of the surface). The annotation of the benchmark is point-based and similarity-based. Hence, for each image, we select several points (Figure 4). We group the points with the exact same materials under the same label. We also define a group of points that have partial similarity. For example, points in group A are more similar to points in group B than to points in group C (in case materials A and B are similar to each other but not identical). This approach captures the complexity of gradual transitions and partial similarities in the world. While also enabling dealing with complex, scattered, and blurry shapes without needing to annotate the full shape, which in many cases is unclear or very hard.

1.3. Main Contributions

This work offers two main contributions in the fields of synthetic data generation and computer vision for materials.

1. In the field of material segmentation, this work offers the first general data set and benchmark for zero-shot segmentation of material states, not restricted to specific materials, states, or environments. This is the first general benchmark dealing with zero-shot and class-agnostic material states segmentation, as well as things like partial similarity and scattered shapes. This task is significantly important to understanding many aspects of the physical world and has a wide range of downstream applications, from cooking and agriculture to controlling chemical experiments and construction^{4,27-34}.
2. In the field of data generation. It offers a general approach to extracting and embedding natural patterns and shapes from the real world into synthetic images in an unsupervised way. Creating synthetic data that can encompass the complexity of the real world is essential for numerous tasks and represents one of the main challenges of machine learning training²³⁻²⁷.

2. Related Works

2.1. Synthetic Data and Domain Gap

Synthetic data and CGI images are extensively used in training machine learning for computer vision⁶⁻²². CGI data is created by combining human-made assets³⁵⁻⁴⁰, simulation, and procedural generation rules. However, synthetic data faces a domain gap and often fails to capture the diversity and complexity of the real world due to the limited diversity of assets and procedural rules¹⁴. To bridge this gap, domain adaptation methods like GAN have been used to adapt the images to different conditions or make them more photorealistic. This, however, mostly focuses on modifying the image and leaving the underlying scene the same, hence having a limited effect on the distribution of the data²³⁻²⁷. Other approaches that combine procedural rules and mathematical functions to better imitate physical reality have been proposed^{14,41}. While the use of natural functions can generate highly complex and realistic scenes, it still has a limited ability to mimic the patterns of the real world using only a set of functions, procedural rules, and handcrafted assets.

2.2. Computer Vision For Materials

Computer vision methods for material recognition include identifying classes, properties, or regions (segments) of materials using cameras or other sensors^{1-5,47,58,60}. This includes classifying materials into different classes⁴²⁻⁴⁶ or using semantic segmentation to split the image into regions belonging to different materials¹⁻⁴. Some methods also quantify specific material properties (e.g., turbidity, glossiness) but are usually restricted to a set of pre-trained properties^{47,48}.

2.3. Zero-Shot and Class Agnostic Methods

Methods for identifying and segmenting materials and textures without being limited to specific pretrained classes or properties are often called one-shot, zero-shot, or class-agnostic. A notable method is CLIP, which can pair almost any image to any text, including material names, with decent accuracy^{21,49,50}. Zero-shot or Class-agnostic segmentation usually receives a query or a point in the image as input and outputs the region of the image that has the same instance or material as the input query (or point)^{7, 8, 9, 22, 52-54}, without being limited to classes used in the training. Some zero-shot/class-agnostic material segmentation approaches were trained on natural images like materials in labs and satellite images, but these were limited to specific domains (chemistry and satellites)^{4,51}. Synthetic data approaches focus on projecting multiple material textures into an image in a random arrangement and generating images with known segmentation maps, which are used to train nets^{7,8,22}. These methods gave good results for simple class-independent materials and texture segmentation^{7,22}. However, the distribution of materials it generates is either random or depends on a set of limited pre-made 3D objects that are generated by humans^{7,8,22}. Both cases don't aim to replicate the complexity of materials in the world, and neither method was tested on material state segmentation. For one-shot recognition, synthetic data have proven very effective for training nets for matching and retrieving specific fine-grain material states and subtypes from various real-world cases using a single example²¹. This implies that simulated PBR materials^{54,55} can be used to train nets to recognize complex real-world material states in a one-shot manner. However, zero-shot material state segmentation methods remain unexplored, partly due to a lack of benchmarks to test this problem.

2. Synthetic Data Generation

The aim of the MatSeg dataset is to capture the diversity and complexity of shapes and patterns formed by material states in the real world while maintaining the precise annotation and scale of synthetic data and to do so in an unsupervised manner and without previous knowledge about the materials or scenes. This includes capturing complex and scattered shapes as well as gradual transitions and soft boundaries. The method shown in Figure 2 is based on automatic harvesting patterns and shapes from natural images and using these to map materials into surfaces of 3D objects in synthetic scenes. The theory is that if we manage to extract a wide enough range of patterns, We will be able to use them to map any material to any object in any environment. And therefore, learn these patterns for the general case.

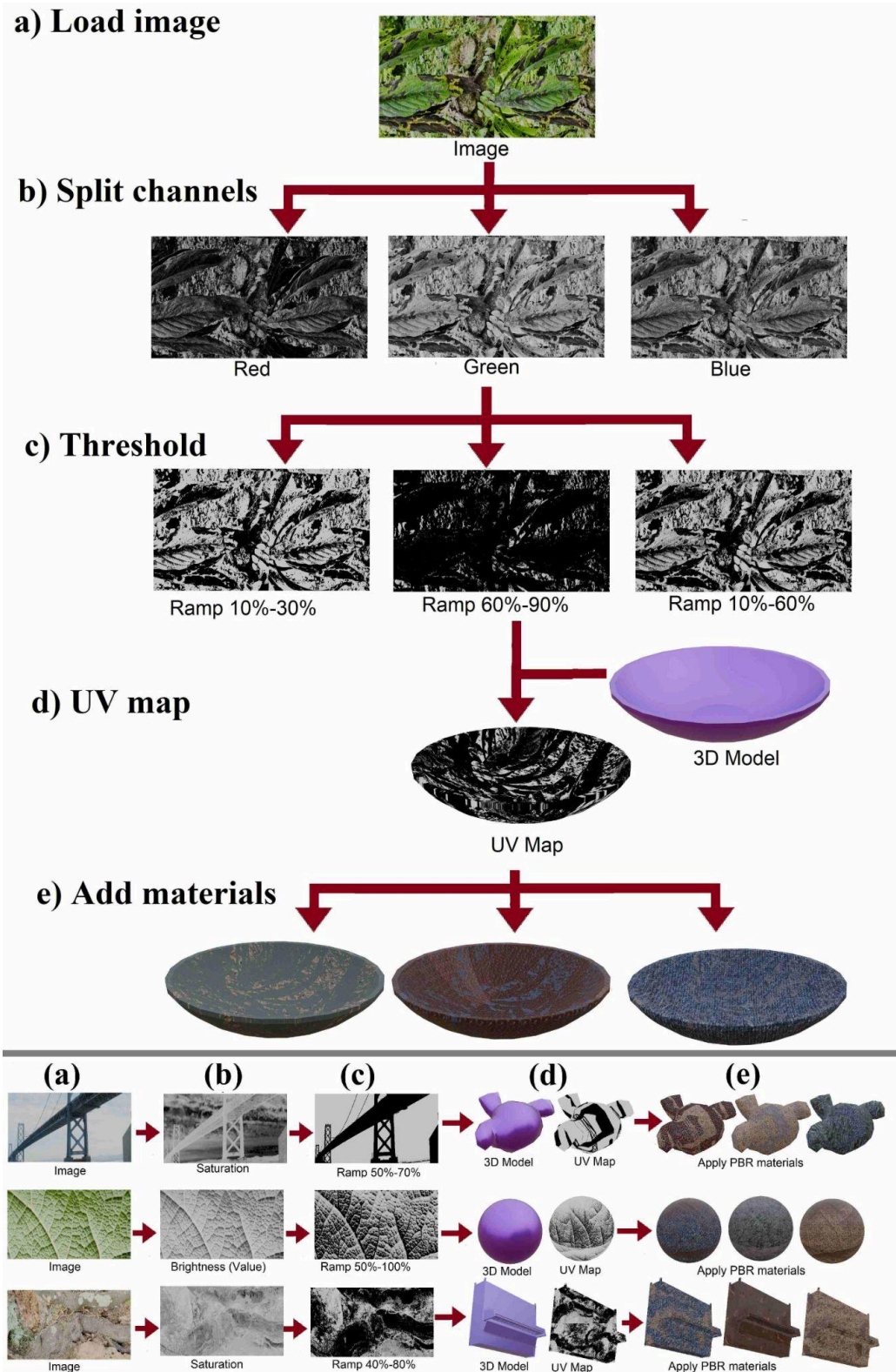


Figure 2) Extracting features from real-world images and mapping them to natural scenes. a) Select a random image. b) Split the image into channels (R,G, B, or H,S,V) and select one channel. c) Apply a fuzzy threshold to the selected channel to get a UV map. d) Select a random 3D object and UV-wrap the map (c) on its surface. e) Select a few random PBR materials and map them to the object surface using the UV map.

3.1. Extracting Shapes and Patterns from Natural Images

The extraction of shapes from natural images involves first randomly picking one property of the image. This can be the saturation, hue, brightness, or one of the red, blue, or green channels (Figure 2b). Each of these features, when normalized, will transform the image into a 2D topological map with values between 0 and 1 for each pixel. The selected map is passed through a fuzzy threshold (color ramp, Figure 2c). This involves picking two random threshold values. Everything above the higher threshold turns 1, everything below the lower threshold turns 0, and everything in between is a linear interpolation between 0 and 1. This allows the map to maintain sharpness while maintaining blurry and gradual transitions. This map can then wrap around the surface of a random object using UV mapping and is used to map different random materials to the object's surface (Figure 2.d,e). Note that when a map has a value of 0.7 at a point, it means that the region will be a mixture of 70% material A and 30% material B. The above approach can easily be used to generate maps for more than two materials by simply applying the splitting again and again in a tree-like structure (using a different map for each split).

3.2. Theoretical Justification

The main assumption in the above approach is that simple image properties like R,G,B, brightness, saturation, or hue can capture the shape and patterns of almost any material state distribution in some cases. Consider, for example, a simple property like brightness (value). It's clear that in some cases, patterns of infected surfaces, suspension in a liquid, mineral in rock, or degradation of the surface will be darker or brighter than their surroundings. For these cases, the brightness map will be a good representation of the material state regions. This correlation between material and a simple property (brightness) will happen only in specific cases. However, assuming we use a large enough set of images and that important patterns appear in many forms and environments, it's likely that they will be correlated with simple properties, at least in some cases. Once captured, patterns can be used to map any material to any object in any scene, allowing the net to learn these patterns for any setting and materials and generalise beyond the setting in which they were extracted. Clearly, many of the patterns that will be captured will have nothing to do with materials. However, this simply means that the distribution will be wider than that of just materials but will still contain the distribution of materials within it.

3.3. Scene Building

Once a UV map is generated, the scene building follows the standard methods described in previous works [21]: 1) Load random 3D objects³⁷⁻⁴⁰. 2) Load random PBR or BSDF^{35,38,54, 55} material for each region of the map and use the generated UV map to set the materials onto the object surface. 3) Load a panoramic HDRI image to act as a background and illumination source³⁶. 4) Add random objects, a ground plane, and sometimes random light sources to create shadows and occlusion in the scene. 5) Set a random camera position and render the image. The scene generation was done procedurally in Blender 4.0⁵⁶. The generation code and the dataset have been made available.

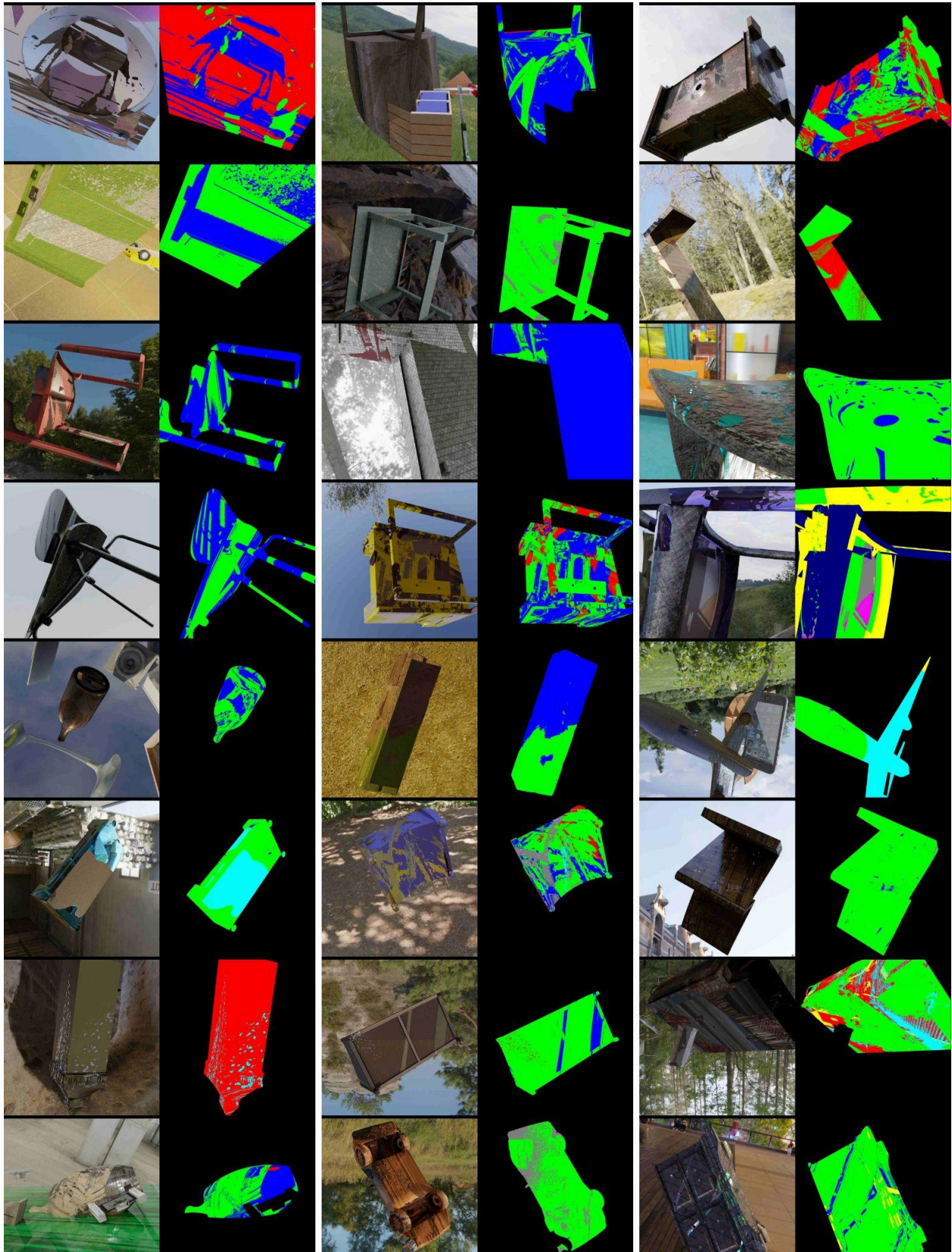


Figure 3) Sample of the synthetic dataset. Each panel shows the rendered image (right) and the corresponding segmentation map (color per material; the black region is the background).

3.4. Materials and Assets Sources

Physics-based rendering (PBR) materials (often named SBRDF^{54,55}) are the main source of realistic textured materials for CGI. Over 4000 PBR textures were downloaded from various open online repositories (FreePBR, TextureBox, AmbientCG)^{35,38}. These were then mixed and combined to create 100,000 new PBR materials. Mixing was done by averaging texture maps of two or more materials, as described in previous works²¹. Textureless (smooth) materials were randomly created by picking a random value for each property (color, transmission, and reflectivity, in the Blender BSDF node⁵⁴⁻⁵⁶). 3D Objects were downloaded from Shapenet and Objaverse, with over 1000000 unique 3D objects³⁷⁻⁴⁰. 600 Panoramics HDRI backgrounds and illuminations were downloaded from HDRI Haven³⁶. Rendering was done in Blender 4 with Cycles rendering⁵⁶.

4. Material State Segmentation Benchmark

The evaluation of any material state segmentation method requires real-world images that capture the diversity and complexity of the material world, both in terms of the images and their annotation (Figure 4). The goal of the benchmark is: 1) Evaluation of the task of material state segmentation in a general class-agnostic way that will be independent of a specific material or setting and cover as much of the material world as possible. 2) Evaluating material states and subtypes with complex, scattered, fuzzy shapes and boundaries (drops, cracks). 3) Evaluating for partial similarity, in which material in one region will be similar but not identical to another region, and gradual transition, in which material gradually changes from one to another. As far as we know, no benchmark is available that tackles these challenges.

4.1. Collecting Images

The images for the benchmark were manually taken from a wide variety of real-world cases, like food at different levels of cooking, liquids with different types of solute and precipitate, minerals on rocks, and sentiment on grounds, landscapes, construction, and others, as well as various processes like wetting, drying, rot, infections, rusting, stains, cracks, and many others (Figure 4). The goal is to capture as much of the world as possible, both in terms of materials and environments (outdoors and indoors). Full manual annotation of images with scatter and soft boundaries is extremely hard, while assigning numerical values for material similarity is, in many cases, impossible. A much easier approach is to sample a few points in the image that represent the main materials' states and their distribution. This allows the annotators to focus on regions with clear annotation but also to sample the harder and more complex regions without the need for too much work or dealing with areas where the segmentation is unclear. The annotation procedure is as follows: 1) Pick points in each image that represent the distribution of each material (Figure 4). 2) Group the points according to their material state such that all points belonging to the same material state will have the same label/group (points of the same color in Figure 4 are in the same group). 3) Assign relative similarity between groups. For example, if material B is a transition state between material A and C we can define points in group A to be more similar to points in group B than to points in group C, and points in group C to be more similar to points in group B than points in group A. Note that points in the same group (same material) always have the highest similarity. This approach circumvents the almost impossible task of assigning numerical similarity to material states (like how cooked food is or how worn metal is). Partial similarity is represented in Figure 4 by setting two dots of different colors

inside a box (top left of each panel), where all points of the same color correspond to the same material state, and two colors in the box imply that these two materials are similar but not identical.

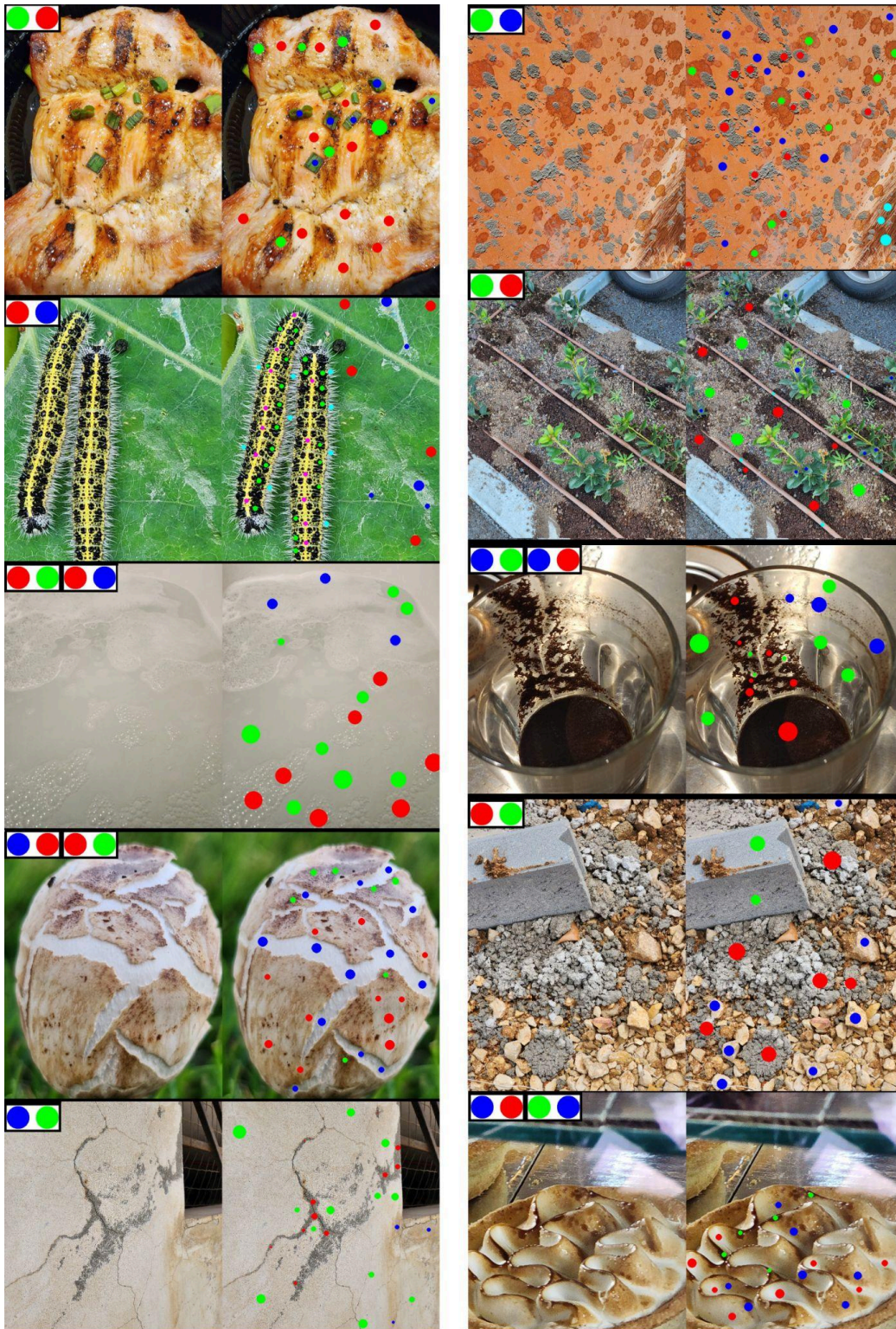


Figure 4) Benchmark samples. The images were annotated using sample points. Dots of the same color on the right panel correspond to the exact same material state. Two or more dots of different colors in a box, in the upper left corner of each panel, imply that the materials (dots) marked by these colors are more similar to each other than to other materials (partial similarity).

5. Evaluation Metrics

The evaluation approach is based on assessing the relative similarity between points in the image. Every segmentation approach, soft or hard, can be easily converted to predict the similarity between two points in the image. For hard segmentation, this similarity will be one if the two points are in the same segment and zero if not. For soft segmentation, the similarity will depend on the similarity map of each segment and point. The triplet evaluation metric is simple: a) We select three points in the image and define one as an anchor. b) We ask which of the remaining two points is more similar to the anchor according to the ground truth (GT) and according to the prediction; if the predictions and GT agree, we assign this as correct. c) If the two points have an identical similarity to the anchor (according to the GT), we ignore this triplet. This is done for all sets of annotated 3 points in the image, and the average is the score (average per material). For this metric, a 50% score means a random guess and a 100% score means perfect segmentation. Note that this metric works both for hard and soft segmentation. We use this metric to evaluate both the net trained on the MatSeg synthetic data as well as a pre-trained materialistic net²² (a recent net that was also trained for material similarity segmentation). Three evaluation modes were used: 1) Hard: only exact similarity (ignore triplets with partial similarity). Soft: only a triplet containing partial similarity between at least one pair. 3) All triplets. The results are given in Table 1. In addition, we also use the TOP 1 metrics, which compare each point to all other points in the image and measure the probability that the most similar point, according to prediction, will belong to the exact same material (according to GT).

5.1. Materialistic Benchmark

Materialistic benchmark is the only one we are aware of for class-agnostic material segmentation [22]. It is limited to 50 images of hard segmentation of different materials on mostly man-made objects (no material states). The materials in this case, usually cover the full object or a bulk region of a wall or structure, with clear, usually straight, boundaries. To evaluate the MatSeg trained net on this benchmark, we select in each material segment a single point and find the similarity of each pixel in the image to the selected point. To turn this into a hard segmentation map, we pick a similarity threshold that maximizes the IOU between the predicted and GT masks of the material. Since the threshold is picked to maximize the IOU, this can be seen as a favorable best-case scenario method. We apply this approach to both the pretrained Materialistic net²² and MatSeg trained net. The results can be seen in Table 1.

6. Net and Training

To test the MatSeg dataset, we use it to train a net for class-agnostic soft material segmentation. Previous works have shown that representing materials in images as vector embeddings and using cosine similarity between these vectors to predict how similar the materials are is an effective method for matching materials states²¹. This representation also has the advantage that it gives soft similarity, which is good for representing mixtures, transition states, and partial similarities. To apply this approach to image segmentation, we use the Unet-style neural net, which predicts 128 long descriptors for each pixel in the image (128-layer output map). This 128-bit vector represents the material for each pixel (Figure 5). The

cosine similarity between vectors of two pixels in the map gives the similarity of the materials in these two pixels. The average vector in a given region (group of pixels) belonging to the same material gives the average vector embedding for this specific material.

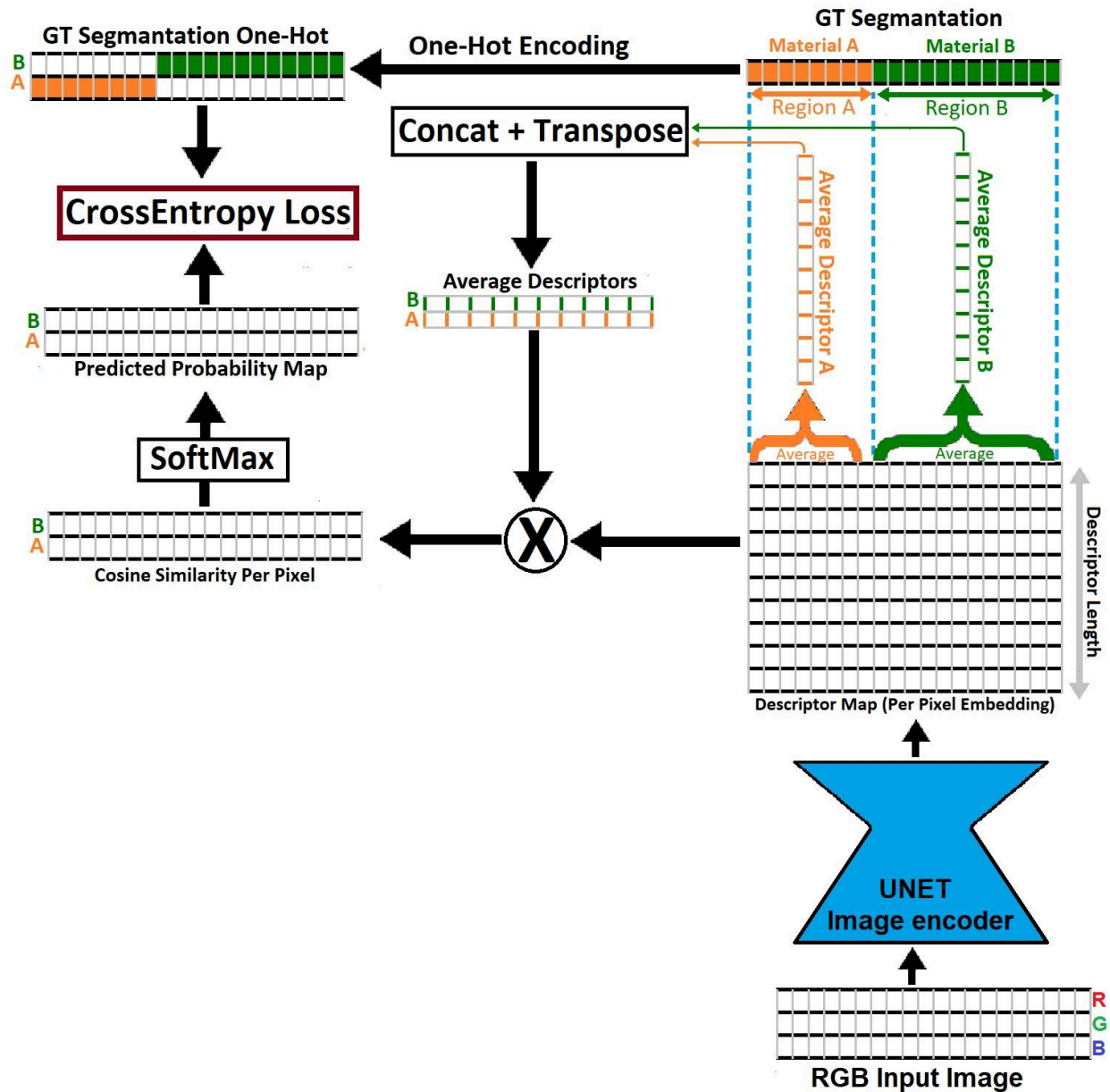


Figure 5) Net and training, a cross-section view. a) The RGB image is passed through the image encoder to create a descriptor map with a vector per pixel. This vector represents the pixel material. b) All the vectors in the region of a given material (based on the GT map) are averaged to create the average descriptor for this material. c) Each individual vector in the predicted descriptor map is matched to the average descriptor of each material in the batch using cosine similarity. This produces a 2D similarity map between each pixel and each material in the batch. d) Stacking the similarity maps and passing them through Softmax gives the predicted material probability map (predicted material per pixel). This map and the GT materials map are used to calculate the final cross-entropy loss.

6.1. Training

The training procedure is depicted in Figure 5 and goes as follows: a) A training batch contains a few randomly sampled images from the MatSeg dataset. b) The images are passed through the net to produce an embedding map with a vector per pixel. These vectors are normalized using L2 normalization. c) The predicted vectors of all the pixels belonging to the same material are averaged to create an average vector per material (Figure 5). To determine which pixels belong to the same material, we use the Ground True (GT) mask of each material and take all the predicted vectors in this region from the descriptor map (Figure 5). e) Each of the average material vectors in the batch is then matched with each vector embedding in the predicted descriptor map. This gives a 2D cosine similarity map between each material in the batch and each pixel in the image. f) The similarity maps for a given image are stacked together and passed through a softmax (temperature of 0.2) to get the probability maps for the match between each pixel in each material. g) These probability maps, along with the GT one-hot masks, are used to calculate a cross-entropy loss. Note that the GT maps are turned from soft to hard (one-hot) segments by selecting for each pixel the GT material with the highest concentration (the highest value according to the GT map).

6.2. Net Architecture and Training Parameters

The net architecture follows that of standard U-net⁵⁹, with a pre-trained ConvNext⁵⁷ base as an encoder, a PSP⁵⁸ layer, and three skip connections upsampling layers (code and training scripts supplied). The training was done using the AdamW optimizer with a learning rate of 1e-5 on a single RTX 3090. The image size was randomly cropped and resized to between 250-900 pixels per dimension. Augmentation includes darkening/lighting, gaussian blurring, partial and full decoloring, and white noise addition. Full code and trained models have been made available.

Table 1: Results of MatSeg trained net and Materialistic (See Sections 4-5 for details).

	MatSeg All (All Triplets) Triplet/Top 1	MatSeg Hard (Exact only) Triplet/Top 1	MatSeg Soft (Partial match only) Triplet/Top 1	Materialistic Test Set (IOU)
MatSeg Trained Net	91%/94%	92%/93%	85%/91%	78%
Materialistic Net	78%/77%	80%/79%	74%/70%	86%
Random	50%/35%	50%/35%	50%/23%	—

7. Results

Results on the MatSeg benchmark are shown in Table 1 and Figures 6-8. Each panel in Figures 6-8 shows an image and the predicted similarity map relative to a selected point in that image, hence how similar the materials in the rest of the image are to the material in the marked point (the selected point is marked as a blue dot, Figure 6-8). It can be seen from Table 1 that the MatSeg-trained net achieves high accuracy across both hard and soft material segmentation, significantly outperforming methods like Materialistic. This is true across a wide range of real-world domains, from rock and construction to food, plants, landscape, fabrics, and liquids (Figure 6-8). Suggesting that the net not only learned to generalize from synthetic to real data but achieved this for a wide range of material states and environments. It can be seen in Figures 6-8 that the net learned to segment sparse and scattered shapes. In addition, the results clearly show the net learned to represent gradual transitions, soft boundaries, and partial similarity between materials. This can be seen by the soft distribution of the similarity maps in Figures 6-8, and the results of the partial similarity measure in Table 1. The MatSeg trained net significantly outperformed the Materialistic net²² across both soft and hard segmentation of the MatSeg benchmark. This is even though both nets were trained on synthetic data. This supports the idea that the natural distribution of patterns in the MatSeg set is far more representative of raw material state distribution in the world. Looking at the samples in Figure 8 it seems that the Materialistic net searches for the boundary of the material based on the boundary of the object and tends to ignore scattered materials on the surface of the object. It also seems to be less sensitive to the material state and more focused on matching materials based on coarse-grain type (Figure 8). This hypothesis is further supported by the fact that the Materialistic net outperformed the MatSeg trained net on the Materialistic test set (Table 1); this test set contains materials with hard boundaries and simple shapes that either encompass the full object (pillows, chairs, cups) or a distinct region with clear and mostly straight boundaries (stairs, wall segments). As such, their shape distribution closely resembles that of man-made assets used in the Materialistic train set or the object boundaries. This implies that using handcrafted shapes and assets for training has an advantage when modeling the distribution of materials on man-made objects or cases where the material covers the full object, while natural patterns of the MatSeg are more representative of raw material states formed by physical processes and states.

7.1. Failure Cases

Analyzing the results in Figure 7 shows the MatSeg-trained net seems to rely more strongly on textures than on shades and colors. This can be seen in the top two center panels in Figure 7, where wet regions with different shades but similar textures are given high similarity. It seems that the net learned to rely on texture above color and shade, likely because texture is more invariant to illumination and shadows. However, this sometimes leads to cases in which the net downplays color and shade-based differences. In most cases, the net manages to mitigate shading and reflection when analyzing material similarity (Figures 6–8). In some cases, things like shadows and reflection still affect the material similarity map (Figure 7, top), suggesting that the net mistaken reflections and shadows to changes in the material composition. It is not fully clear why, in some cases, the net manages to account for reflection and shadows and, in others, less so. It seems that in cases like landscapes and very large scenes, the net is more vulnerable to these issues, while highly reflective materials are more likely to reflect patterns that will be mistaken for different materials.

7.2. Can The Segment Anything Model (SAM) Segment Materials?

Segment Anything Model (SAM)⁵³ is a class-independent segmentation net that was trained on a vast amount of manually annotated data (11 million images, 1 billion masks), to be able to segment anything. The net receives one or more points in the image and predicts the mask of the segment containing these points. It can also receive negative points for where the segment should not be. SAM is not focused on materials and therefore is not expected to segment the material based on a single point and likely needs several positive and negative points to guide it. However, the results (Figure 9) show that when dealing with sparse or scattered materials, SAM is unable to segment the scattered material even after having multiple negative and positive points as input. Hence, despite training on a mass amount of real-world images, it was not able to learn to generalize for sparse materials. SAM does well when the material is localized into one bulk segment (Figure 9, bottom right). Suggesting that SAM does understand materials as a way to cluster connected regions but not the similarity between materials in different regions. The focus of SAM training data on manual annotation, in which it is very hard to annotate scattered shapes, might explain this limitation.

8. Conclusion

Understanding and capturing the complexity of materials in the world is fundamental to understanding the physical world. This work makes two major contributions to this field. First by demonstrating a method for capturing complex patterns from the real world and implanting them in synthetic data. Creating synthetic data that captures the complexity of the natural world is essential for providing the vast amount of training data needed for deep learning methods. A second contribution to the work is presenting the first zero-shot benchmark for general material state segmentation. This benchmark captures both soft and hard segmentation of material states from a wide range of real-world examples and deals with sparse, scattered, complex, and soft boundaries and gradual transitions that were ignored in previous segmentation materials benchmarks. Those open the way for a broader view of material segmentation beyond what was possible with previous benchmarks.

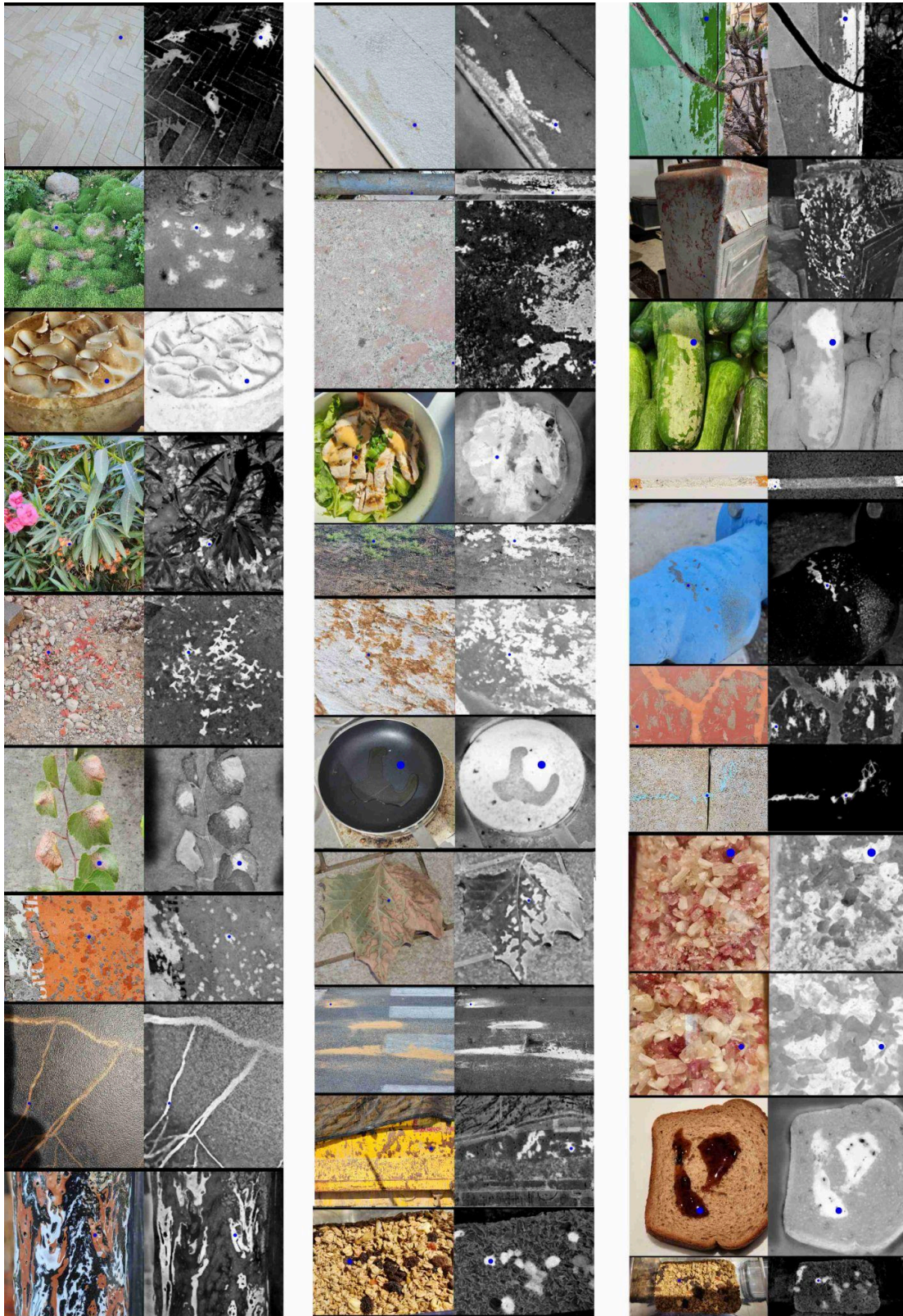


Figure 6. Results of the MatSeg-trained net on the MatSeg Benchmark. Each panel shows an image (left) with a selected point (blue dot). And the predicted material similarity of all other pixels to the material on the dot (right). Bright regions imply high similarity.

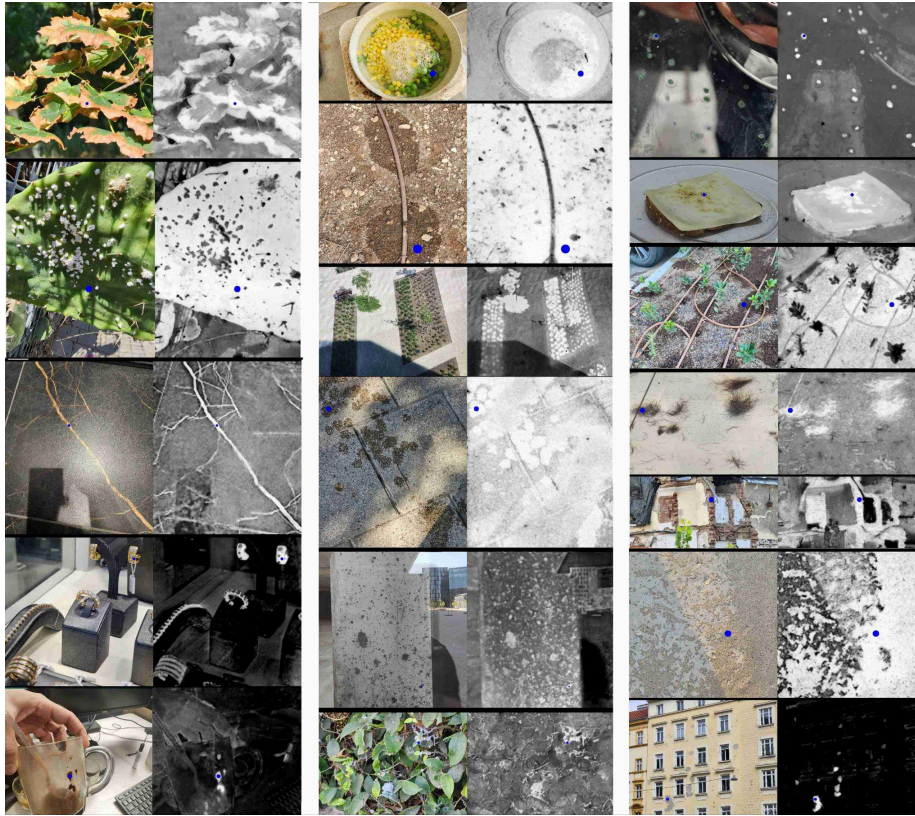


Figure 7. Results of the MatSeg-trained net on the MatSeg benchmark, with hard examples and failure cases. Each panel shows an image (left) with a selected point (blue dot). And the predicted material similarity of all other pixels to the material on the dot (right). Bright regions imply high similarity.

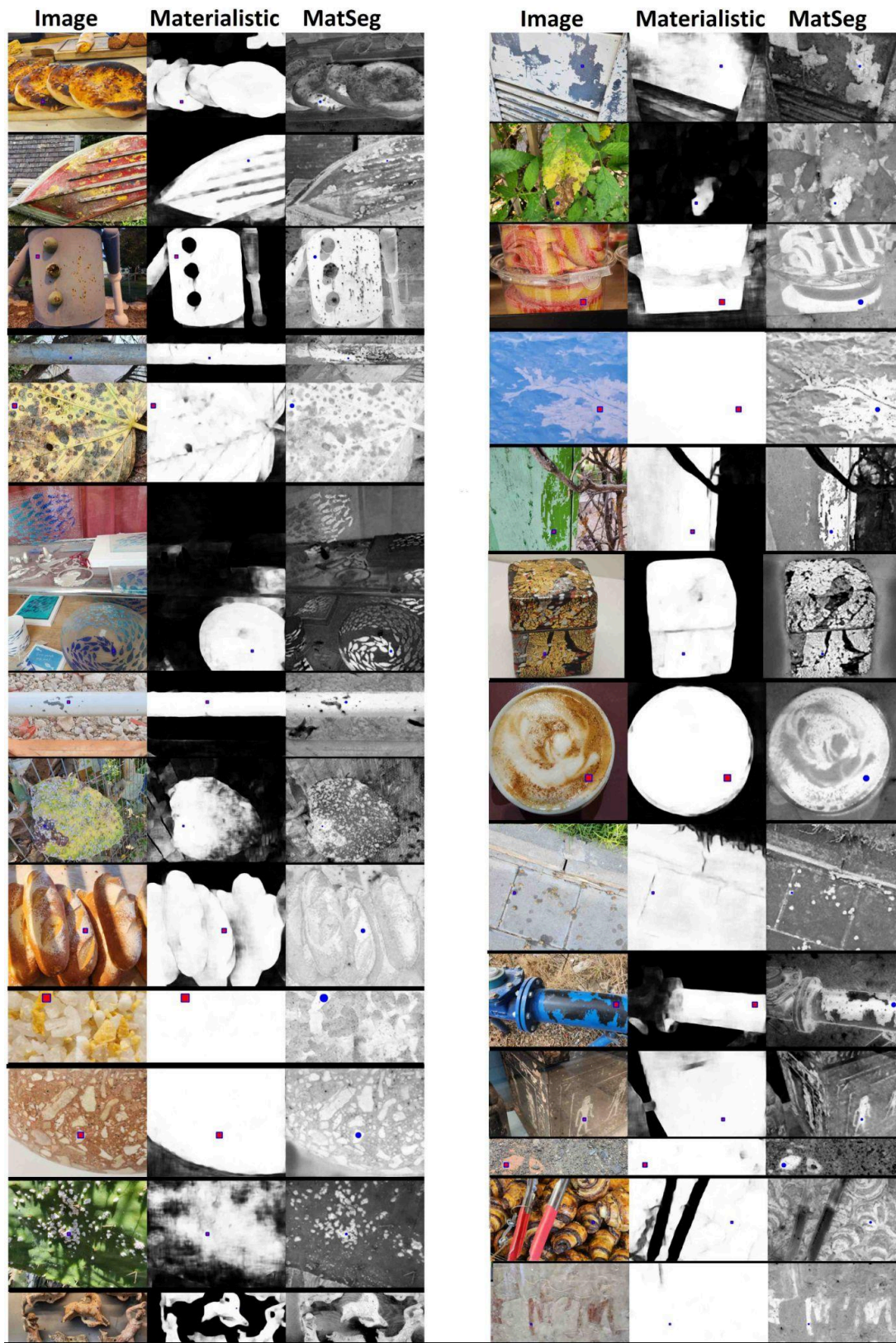


Figure 8. Predicted similarity map of the materials in the image (Left) to the red/blue point for the pre-trained Materialistic net (Center) and MatSeg trained net (Right).



Figure 9. Results of the Segment Anything Model (SAM). Light blue points are positive input for the net (where the segment should be). Pink points are negative input (where the mask should not be). Regions segmented by the net are outlined blue (and are brighter). It can be seen that for scattered materials, despite being given multiple positive and negative points as input, the net fails to segment the material region. For material in one large connected component (bottom right), SAM works well with only a few input points.

9. References

1. Bell, Sean, et al. "OpenSurfaces: A Richly Annotated Catalog of Surface Appearance." *ACM Transactions on Graphics (TOG)*, vol. 32, no. 4, 2013, pp. 1–17.
2. Bell, Sean, et al. "Material Recognition in the Wild with the Materials in Context Database." *Proceedings of the IEEE Conference on Computer Vision and Pattern Recognition*, 2015, pp. 3479–3487.
3. Upchurch, Paul, and Ransen Niu. "A Dense Material Segmentation Dataset for Indoor and Outdoor Scene Parsing." *Computer Vision–ECCV 2022: 17th European Conference, Tel Aviv, Israel, October 23–27, 2022, Proceedings, Part VIII*, Springer, 2022, pp. 450–466.
4. Eppel, Sagi, et al. "Computer Vision for Recognition of Materials and Vessels in Chemistry Lab Settings and the Vector-LabPics Data Set." *ACS Central Science*, vol. 6, no. 10, 2020, pp. 1743–1752.
5. Aksoy, Yağiz, et al. "Semantic soft segmentation." *ACM Transactions on Graphics (TOG)* 37.4 (2018): 1-13.
6. Haindl, Michal, and Stanislav Mikes. "Texture segmentation benchmark." *2008 19th International Conference on Pattern Recognition*. IEEE, 2008.
7. Ustyuzhaninov, Ivan, et al. "One-shot texture segmentation." *arXiv preprint arXiv:1807.02654* (2018).
8. Soares, Lucas de Assis, et al. "A class-independent texture-separation method based on a pixel-wise binary classification." *Sensors* 20.18 (2020): 5432.
9. Chen, Yu, et al. "A Self-Supervised Miniature One-Shot Texture Segmentation (MOSTS) Model for Real-Time Robot Navigation and Embedded Applications." *arXiv preprint arXiv:2306.08814* (2023).
10. Andrearczyk, Vincent, and Paul F. Whelan. "Texture segmentation with fully convolutional networks." *arXiv preprint arXiv:1703.05230* (2017).
11. Nikolenko, Sergey I. "Synthetic data for deep learning." *arXiv preprint arXiv:1909.11512* (2019).
12. Stets, Jonathan Dyssel, et al. "Material-based segmentation of objects." *Image Analysis: 21st Scandinavian Conference, SCIA 2019, Norrköping, Sweden, June 11–13, 2019, Proceedings 21*. Springer International Publishing, 2019.
13. Song, Jian, Hongrui Xuan Chen, and Naoto Yokoya. "SyntheWorld: A Large-Scale Synthetic Dataset for Land Cover Mapping and Building Change Detection." *Proceedings of the IEEE/CVF Winter Conference on Applications of Computer Vision*. 2024.

14. Raistrick, Alexander, et al. "Infinite Photorealistic Worlds using Procedural Generation." *Proceedings of the IEEE/CVF Conference on Computer Vision and Pattern Recognition*. 2023.
15. Richter, Stephan R., et al. "Playing for data: Ground truth from computer games." *Computer Vision—ECCV 2016: 14th European Conference, Amsterdam, The Netherlands, October 11–14, 2016, Proceedings, Part II 14*. Springer International Publishing, 2016.
16. Stets, Jonathan Dyssel, et al. "Material-based segmentation of objects." *Image Analysis: 21st Scandinavian Conference, SCIA 2019, Norrköping, Sweden, June 11–13, 2019, Proceedings 21*. Springer International Publishing, 2019.
17. Ingebo, Ole Martin. *Generation and Evaluation of Realistic Training Image Data for Machine Learning-Based Crack Detection*. MS thesis. NTNU, 2023.
18. Roberts, Mike, et al. "Hypersim: A photorealistic synthetic dataset for holistic indoor scene understanding." *Proceedings of the IEEE/CVF international conference on computer vision*. 2021.
19. Perroni-Scharf, Maxine, et al. "Material Swapping for 3D Scenes Using a Learnt Material Similarity Measure." *Proceedings of the IEEE/CVF Conference on Computer Vision and Pattern Recognition*, 2022, pp. 2034–2043.
20. Lagunas, Manuel, et al. "A Similarity Measure for Material Appearance." *arXiv preprint arXiv:1905.01562*, 2019.
21. Drehwald, Manuel S., et al. "One-shot recognition of any material anywhere using contrastive learning with physics-based rendering." *arXiv e-prints* (2022): arXiv:2212.
22. Sharma, Prafull, et al. "Materialistic: Selecting Similar Materials in Images." *arXiv preprint arXiv:2305.13291* (2023).
23. Eversberg, Leon, and Jens Lambrecht. "Generating Images with Physics-Based Rendering for an Industrial Object Detection Task: Realism Versus Domain Randomization." *Sensors*, vol. 21, no. 23, 2021, 7901.
24. Reddy, Arun V., et al. "Synthetic-to-real domain adaptation for action recognition: A dataset and baseline performances." *arXiv preprint arXiv:2303.10280* (2023)
25. Sankaranarayanan, Swami, et al. "Generate to adapt: Aligning domains using generative adversarial networks." *Proceedings of the IEEE conference on computer vision and pattern recognition*. 2018.
26. Zhao, Sicheng, et al. "A review of single-source deep unsupervised visual domain adaptation." *IEEE Transactions on Neural Networks and Learning Systems* 33.2 (2020): 473-493.
27. James, Stephen, et al. "Sim-to-real via sim-to-sim: Data-efficient robotic grasping via randomized-to-canonical adaptation networks." *Proceedings of the IEEE/CVF Conference on Computer Vision and Pattern Recognition*. 2019.
28. Andrearczyk, Vincent, and Paul F. Whelan. "Deep learning in texture analysis and its application to tissue image classification." *Biomedical texture analysis*. Academic Press, 2017. 95-129.
29. Chen, Yu, et al. "A Self-Supervised Miniature One-Shot Texture Segmentation (MOSTS) Model for Real-Time Robot Navigation and Embedded Applications." *arXiv preprint arXiv:2306.08814* (2023).
30. Zheng, Junwei, et al. "MATERobot: Material Recognition in Wearable Robotics for People with Visual Impairments." *arXiv preprint arXiv:2302.14595* (2023).
31. Ardelean, Andrei-Timotei, and Tim Weyrich. "High-Fidelity Zero-Shot Texture Anomaly Localization Using Feature Correspondence Analysis." *Proceedings of the IEEE/CVF Winter Conference on Applications of Computer Vision*. 2024.
32. Ingebo, Ole Martin. *Generation and Evaluation of Realistic Training Image Data for Machine Learning-Based Crack Detection*. MS thesis. NTNU, 2023.
33. Brilakis, Ioannis K., Lucio Soibelman, and Yoshihisa Shinagawa. "Construction Site Image Retrieval Based on Material Cluster Recognition." *Advanced Engineering Informatics*, vol. 20, no. 4, 2006, pp. 443–452.
34. Choudhary, Kamal, et al. "Recent advances and applications of deep learning methods in materials science." *npj Computational Materials* 8.1 (2022): 59.
35. "AmbientCG." *AmbientCG*, <https://ambientcg.com/>. Accessed 1 Mar. 2024.
36. "Polyhaven." *Polyhaven*, <https://polyhaven.com>. Accessed 1 Mar. 2024.

37. Chang, Angel X., et al. "ShapeNet: An Information-Rich 3D Model Repository." *arXiv preprint arXiv:1512.03012*, 2015.
38. Zraggen, Dorian. "CGBookcase Free PBR Textures Library." <https://www.cgbookcase.com/>
39. Deitke, Matt, et al. "Objaverse-xl: A universe of 10m+ 3d objects." *Advances in Neural Information Processing Systems* 36 (2024).
40. Deitke, Matt, et al. "Objaverse: A universe of annotated 3d objects." *Proceedings of the IEEE/CVF Conference on Computer Vision and Pattern Recognition*. 2023.
41. Carroll, Sean B. *Endless forms most beautiful: The new science of evo devo and the making of the animal kingdom*. No. 54. WW Norton & Company, 2005.
42. Cimpoi, Mircea, et al. "Describing textures in the wild." *Proceedings of the IEEE conference on computer vision and pattern recognition*. 2014.
43. L. Sharan, R. Rosenholtz, and E. H. Adelson, "Accuracy and speed of material categorization in real-world images", *Journal of Vision*, vol. 14, no. 9, article 12, 2014 [BibTex]
44. C. Liu, L. Sharan, E. H. Adelson, and R. Rosenholtz, "Exploring features in a Bayesian framework for material recognition", in *Proc. of IEEE Conference on Computer Vision and Pattern Recognition (CVPR)*, pp. 239-246, 2010
45. L. Sharan, C. Liu, R. Rosenholtz, and E. H. Adelson, "Recognizing materials using perceptually inspired features", *International Journal of Computer Vision*, vol. 108, no. 3, pp. 348-371, 2013
46. Hayman, Eric, et al. "On the Significance of Real-World Conditions for Material Classification." *European Conference on Computer Vision*, Springer, 2004, pp. 253–266.
47. Pizzuto, Gabriella, et al. "Solis: Autonomous solubility screening using deep neural networks." *2022 International Joint Conference on Neural Networks (IJCNN)*. IEEE, 2022.
48. Chadwick, Alice C., and R.W. Kentridge. "The Perception of Gloss: A Review." *Vision Research*, vol. 109, 2015, pp. 221–235.
49. Radford, Alec, et al. "Learning Transferable Visual Models from Natural Language Supervision." *International Conference on Machine Learning*, PMLR, 2021, pp. 8748–8763.
50. Schuhmann, Christoph, et al. "LAION-5B: An Open Large-Scale Dataset for Training Next Generation Image-Text Models." *arXiv preprint arXiv:2210.08402*, 2022.
51. Akiva, Peri, Matthew Purri, and Matthew Leotta. "Self-supervised material and texture representation learning for remote sensing tasks." *Proceedings of the IEEE/CVF Conference on Computer Vision and Pattern Recognition*. 2022.
52. Eppel, Sagi. "Class-independent sequential full image segmentation, using a convolutional net that finds a segment within an attention region, given a pointer pixel within this segment." *arXiv preprint arXiv:1902.07810* (2019).
53. Kirillov, Alexander, et al. "Segment anything." *arXiv preprint arXiv:2304.02643* (2023).
54. Bartell, Frederick O., Eustace L. Dereniak, and William L. Wolfe. "The Theory and Measurement of Bidirectional Reflectance Distribution Function (BRDF) and Bidirectional Transmittance Distribution Function (BTDF)." *Radiation Scattering in Optical Systems*, vol. 257, SPIE, 1981, pp. 154–160.
55. Pharr, Matt, Wenzel Jakob, and Greg Humphreys. *Physically Based Rendering: From Theory to Implementation*. Morgan Kaufmann, 2016.
56. blender.org Community. "Blender: A 3D Modelling and Rendering." <https://www.blender.org/>.
57. Liu, Zhuang, et al. "A ConvNet for the 2020s." *Proceedings of the IEEE/CVF Conference on Computer Vision and Pattern Recognition*, 2022, pp. 11976–11986.
58. Zhao, Hengshuang, et al. "Pyramid scene parsing network." *Proceedings of the IEEE conference on computer vision and pattern recognition*. 2017.
59. Ronneberger, Olaf, Philipp Fischer, and Thomas Brox. "U-net: Convolutional networks for biomedical image segmentation." *Medical Image Computing and Computer-Assisted Intervention–MICCAI 2015: 18th International Conference, Munich, Germany, October 5-9, 2015, Proceedings, Part III* 18. Springer International Publishing, 2015.

60. Dhahri, Ahmed, et al. "Surface multi-spectral reflectivity and texture material recognition in non-constrained environments." (2024).